

1 **REPEAT EXPOSURE TO HYPERCAPNIC SEAWATER MODIFIES PERFORMANCE**
2 **AND OXIDATIVE STATUS IN A TOLERANT BURROWING CLAM**

3

4 **Running title:** Repeat $p\text{CO}_2$ stress and geoduck response

5

6 **Samuel J. Gurr^{1*}, Shelly A. Trigg³, Brent Vadopalas², Steven B. Roberts³, Hollie M. Putnam¹**

7

8 ¹University of Rhode Island, College of the Environment and Life Sciences, 120 Flagg Rd,
9 Kingston, RI 02881 USA

10 ²University of Washington, Washington Sea Grant, 3716 Brooklyn Ave NE, Seattle, WA 98105
11 USA

12 ³University of Washington, School of Aquatic and Fishery Sciences, 1122 NE Boat St, Seattle,
13 WA 98105 USA

14

15 **Corresponding author:** Samuel J. Gurr; 120 Flagg Rd, Kingston, RI 02881 USA,

16 samuel_gurr@uri.edu

17

18 **Keywords:** hormesis, ocean acidification, oxidative stress, phenotypic variation, stress
19 acclimation, geoduck

20

21 **Summary statement:** Hypercapnic conditions during postlarval development improves
22 physiological performance and oxidative status. This novel investigation of adaptive stress
23 acclimation highlights the plasticity of bioenergetic and subcellular responses in *Panopea*
24 *generosa*.

25

26

27

28

29

30

31

32 **Abstract**

33 Moderate oxidative stress is a hypothesized driver of enhanced stress tolerance and lifespan.
34 Whereas thermal stress, irradiance, and dietary restriction show evidence of dose-dependent
35 benefits for many taxa, stress acclimation remains understudied in marine invertebrates, despite
36 being threatened by climate change stressors such as ocean acidification. To test for life-stage and
37 stress-intensity dependence in eliciting enhanced tolerance under subsequent stress encounters, we
38 initially conditioned pediveliger Pacific geoduck (*Panopea generosa*) larvae to (i) ambient and
39 moderately elevated $p\text{CO}_2$ (920 μatm and 2800 μatm , respectively) for 110 days, (ii) secondarily
40 applied a 7-day exposure to ambient, moderate, and severely elevated $p\text{CO}_2$ (750 μatm , 2800 μatm ,
41 and 4900 μatm , respectively), followed by 7 days in ambient conditions, and (iii) implemented a
42 modified-reciprocal 7-day tertiary exposure to ambient (970 μatm) and moderate $p\text{CO}_2$ (3000
43 μatm). Initial conditioning to moderate $p\text{CO}_2$ stress followed by secondary and tertiary exposure
44 to severe and moderate $p\text{CO}_2$ stress increased respiration rate, organic biomass, and shell size
45 suggesting a stress-intensity-dependent effect on energetics. Additionally, stress-acclimated clams
46 had lower antioxidant capacity compared to clams under initial ambient conditions, supporting the
47 hypothesis that stress over postlarval-to-juvenile development affects oxidative status later in life.
48 We posit two subcellular mechanisms underpinning stress-intensity-dependent effects on
49 mitochondrial pathways and energy partitioning: i) stress-induced attenuation of mitochondrial
50 function and ii) adaptive mitochondrial shift under moderate stress. Time series and stress
51 intensity-specific approaches can reveal life-stages and magnitudes of exposure, respectively, that
52 may elicit beneficial phenotypic variation.

53

54

55

56

57

58

59

60

61

62

63 1. Introduction

64 Ocean acidification (OA), or the decrease of oceanic pH, carbonate ion concentration, and
65 aragonite saturation (Ω) due to elevated atmospheric partial pressures ($p\text{CO}_2$), poses a global threat
66 with magnified intensity in coastal marine systems (Cai et al., 2011). Marine molluscs are
67 particularly susceptible to OA, with negative physiological impacts in aerobic performance
68 (Navarro et al., 2013), calcification, growth and development (Waldbusser et al., 2015), acid/base
69 regulation (Michaelidis et al., 2005), and energy-consuming processes (i.e. protein synthesis; Pan
70 et al., 2015).

71 Principles in ectotherm physiology (i.e. oxygen capacity-limited thermal tolerance:
72 Pörtner, 2012; energy-limited tolerance to stress: Sokolova, 2013) describe aerobic performance
73 “windows” under ‘optimum’, ‘pejus’ (moderate), and ‘pessimum’ (severe) environmental ranges
74 defined by cellular and physiological modifications affecting energy homeostasis (Sokolova et al.,
75 2012). The conserved defense proteome, or cellular stress response (CSR), is the hallmark of
76 cellular protection but comes at an energetic cost (Kültz, 2005). Whereas the CSR is unsustainable
77 if harmful conditions exacerbate or persist (Sokolova et al., 2012), episodic or sublethal stress
78 encounters can induce adaptive phenotypic variation (Tanner and Dowd, 2019). A growing body
79 of research suggests moderate or intermittent stress (e.g. caloric restriction, irradiance, thermal
80 stress, oxygen deprivation, etc.) can elicit experience-mediated resilience for a variety of taxa (i.e.
81 fruit fly, coral, fish, zebra finch, mice) increasing CSR, fitness, and compensatory/anticipatory
82 responses under subsequent stress exposures (Brown et al., 2002; Costantini et al., 2012; Jonsson
83 and Jonsson, 2014; Visser et al., 2018; Zhang et al., 2018). Further, early-life development presents
84 a sensitive stage to elicit adaptive phenotypic adjustments (Fawcett and Frankenhuys, 2015)
85 prompting investigation of environmental stress acclimation under a rapidly changing
86 environment.

87 Dose-dependent stress response, or conditioning-hormesis (Calabrese et al., 2007),
88 explains how stress priming can enhance tolerance limitations under subsequent encounters to
89 similar or higher levels of stress intensity later in life (Costantini, 2014). Oxidative stress presents
90 a common source of conditioning-hormesis (Costantini, 2014) and is a hypothesized driver of
91 longevity (Ristow and Schmeisser, 2014; Wojtczyk-Miaskowska and Schlichtholz, 2018). For
92 example, early-life exposure to moderate oxidative stress in the Caribbean fruit fly *Anastrepha*
93 *suspensa* and zebra finch *Taeniopygia guttata* decreases cellular damage and increases proteomic

94 defense, energy assimilation, and survival under a subsequent stress encounter during adulthood
95 (Costantini et al., 2012; Visser et al., 2018). Oxidative stress, or an over-production of reactive
96 oxygen species (ROS; superoxide, hydrogen peroxide, hydroxyl radical) primarily from
97 mitochondrial oxidative phosphorylation, causes macromolecular damage. In marine
98 invertebrates, oxidative stress can intensify under environmental stressors such as hypoxia and
99 emersion (Abele et al., 2008), hyposalinity (Tomanek et al., 2012), thermal stress (An and Choi,
100 2010), pollutants and contaminants (Livingstone, 2001), and OA (Tomanek et al., 2011; Matoo et
101 al., 2013). Protein families that are involved in the CSR, function in signaling, avoidance, and
102 mediation of oxidative damage. Specifically, antioxidant proteins (i.e. superoxide dismutase,
103 catalase, glutathione peroxidase, etc.) are widely conserved across phyla to scavenge ROS and
104 ameliorate redox status at the expense of energy homeostasis (Kültz, 2005). Adaptive cellular
105 defense against oxidative damage is thought to have an important evolutionary role in the longevity
106 of the ocean quahog *Arctica islandica* (lifespan > 400 years) due to a lifestyle of metabolic
107 dormancy (when burrowed) and aerobic recovery (Abele et al., 2008). Further, Ivanina and
108 Sokolova (Ivanina and Sokolova, 2016) found hypoxia-tolerant marine bivalves show anticipatory
109 and compensatory upregulation of antioxidant proteins to mitigate oxidative bursts under hypoxia-
110 reoxygenation. Such adaptive responses have yet to be explored under hypercapnic conditions to
111 identify species tolerant to OA stress. Although bivalves are known to exhibit $p\text{CO}_2$ -induced
112 oxidative damage and upregulated CSR (Tomanek et al., 2011; Matoo et al., 2013), studies have
113 yet to investigate ROS-mediated activity in a hormetic framework (repeated dose exposures).

114 Pacific geoduck (*Panopea generosa*) are burrowing clams of ecological (Goodwin and
115 Pease, 1987) and economic importance (Shamshak and King, 2015) and are a great candidate for
116 investigating a hormetic framework for generation of stress-acclimated phenotypes. Juvenile
117 geoduck have shown positive carryover effects after exposures under high $p\text{CO}_2$ /low Ω conditions
118 including compensatory respiration rates and shell growth (Gurr et al., 2020). In contrast, larval
119 performance is negatively impacted under OA exposure (Timmins-Schiffman et al., 2020). The
120 postlarval life stage presents an ecologically relevant and less susceptible window to investigate
121 effects of $p\text{CO}_2$ stress acclimation. ‘Settlement’ in bivalves is a developmental transition from
122 free-swimming larvae in an oxygen-saturated water column to an increasingly sedentary or
123 burrowed life in the benthos (Goodwin and Pease, 1989) where stratification, bacterial carbon
124 mineralization, and reduced buffering capacity drives down aragonite saturation and oxygen (Cai

125 et al., 2011). To investigate thresholds of hormesis and potential for beneficial stress acclimation,
126 we investigated the effects of $p\text{CO}_2$ exposures of different intensity and at different time points in
127 a repeated reciprocal fashion, on the physiological and subcellular phenotypes of juvenile Pacific
128 geoduck.

129

130 **2. Materials and Methods**

131 **2.1 Experimental setup**

132 Larval Pacific geoduck were reared from gametes at the Jamestown Point Whitney
133 Shellfish Hatchery (Brinnon, WA) following standard shellfish aquaculture industry practices,
134 using bag-filtered ($5\mu\text{m}$) and UV sterilized seawater pumped from offshore (27.5 m depth) in
135 Dabob Bay (WA, USA). Ambient seawater temperature, salinity, pH, and $p\text{CO}_2$ was 16-18 °C, 29
136 ppt, 7.7-7.8 pH, and $\sim 800\text{-}950\ \mu\text{atm}$, respectively. Larvae reached settlement competency,
137 characterized by a protruding foot and larval shell length $>300\ \mu\text{m}$, at 30 days post-fertilization.
138 Approximately 15,000 larvae were randomly placed into each of eight 10-L trays (Heath/Tecna)
139 containing a thin layer of sand to simulate the natural environment and enable metamorphosis from
140 veliger larvae to pediveliger larvae, and subsequently to the burrowing and sessile juvenile stage.

141 **2.2 Acclimation from pediveligers to juveniles**

142 Initial Exposure (110 days): Pediveligers were placed into ambient and elevated $p\text{CO}_2$
143 conditions ($921 \pm 41\ \mu\text{atm}$ and $2870 \pm 65\ \mu\text{atm}$; Table 1; Fig. 1) for an initial exposure during the
144 transition from pediveliger to the burrowing juvenile stage ($N=4$ trays treatment⁻¹; $N=1.5 \times 10^4$
145 pediveligers tray⁻¹). Seawater flowed into 250-L head tanks at a rate of $0.1\ \text{L min}^{-1}$ and replicate
146 trays were gravity-fed from the head tanks. At the end of the initial exposure, respiration rate and
147 shell growth was measured for 20 randomly selected juveniles from each of the eight trays as
148 described below. Additionally, six animals from each tray were frozen in liquid nitrogen and stored
149 at $-80\ ^\circ\text{C}$ for molecular analyses.

150

151

152

153

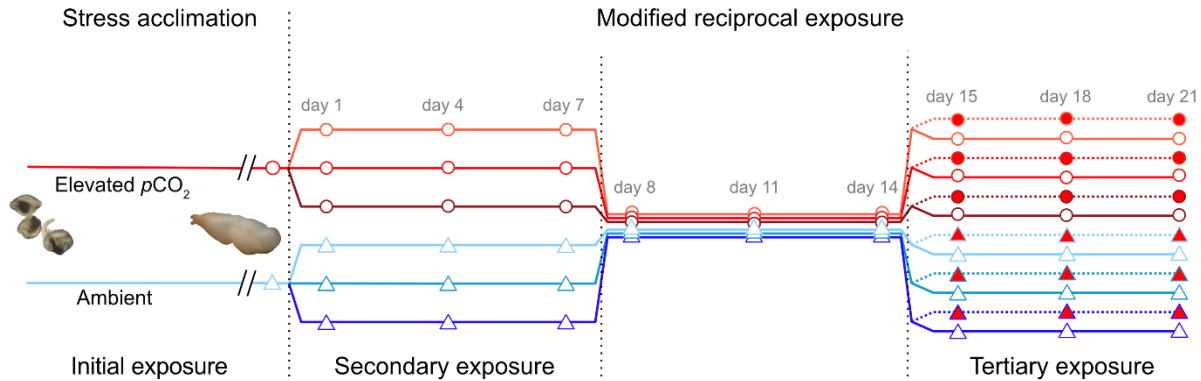
154

155 **Table 1. Seawater carbonate chemistry.** pH, salinity, and temperature measured with handheld
 156 probes and total alkalinity (via Gran titration) measured with 60 mL from trays and tanks during
 157 the 110-day acclimation period (weekly) and during the 21-day experiment, respectively. Seawater
 158 carbonate chemistry (CO_2 , $p\text{CO}_2$, HCO_3^- , CO_3^{2-} , DIC, aragonite saturation state) was calculated
 159 with the seacarb R package (Gattuso et al., 2018).
 160

Treatment	N	Salinity	Temperature	pH, Total Scale	CO_2 $\mu\text{mol kg}^{-1}$	$p\text{CO}_2$ μatm	HCO_3^- $\mu\text{mol kg}^{-1}$	CO_3^{2-} $\mu\text{mol kg}^{-1}$	DIC $\mu\text{mol kg}^{-1}$	Total Alkalinity $\mu\text{mol kg}^{-1}$	Aragonite Saturation state
Initial exposure (3-month conditioning)											
Ambient	27	29.3 ± 0.0426	16.8 ± 0.192	7.7 ± 0.0187	33.5 ± 1.36	921 ± 40.7	1850 ± 8.09	64.9 ± 2.6	1950 ± 7.63	2010 ± 6.55	1.02 ± 0.0405
Elevated	24	29.3 ± 0.0448	17.3 ± 0.205	7.22 ± 0.00921	103 ± 2.24	2870 ± 64.7	1950 ± 5.26	22.9 ± 0.454	2070 ± 6.09	2010 ± 5.29	0.361 ± 0.00722
Secondary exposure											
Ambient	33	29.2 ± 0.009	17.6 ± 0.087	7.78 ± 0.00777	27 ± 0.57	754 ± 15	1850 ± 4.81	79.1 ± 1.37	1950 ± 4.13	2040 ± 2.26	1.25 ± 0.0217
Moderate	33	29.2 ± 0.0138	17.6 ± 0.0895	7.24 ± 0.00467	98.1 ± 0.881	2750 ± 31.1	1980 ± 2.21	24.8 ± 0.195	2110 ± 2.5	2040 ± 2.46	0.392 ± 0.00295
Severe	33	29.2 ± 0.00833	17.6 ± 0.0862	7 ± 0.00416	176 ± 1.58	4940 ± 44.6	2010 ± 1.53	14.2 ± 0.143	2200 ± 2.57	2050 ± 1.77	0.225 ± 0.00228
Ambient recovery period											
Ambient	80	29.1 ± 0.0102	18.2 ± 0.0428	7.71 ± 0.00499	31.4 ± 0.392	896 ± 10.7	1890 ± 2.93	71.2 ± 0.822	1990 ± 2.5	2060 ± 1.18	1.13 ± 0.0132
Tertiary exposure											
Ambient	46	29.3 ± 0.0138	17.7 ± 0.0779	7.68 ± 0.00364	34.5 ± 0.368	967 ± 8.95	1920 ± 4.64	66.4 ± 0.609	2020 ± 4.66	2080 ± 4.09	1.05 ± 0.01
Moderate	45	29.2 ± 0.0156	17.8 ± 0.0596	7.21 ± 0.00311	108 ± 0.832	3030 ± 22.5	2020 ± 3.28	23.5 ± 0.165	2150 ± 3.76	2080 ± 3.22	0.372 ± 0.00262

161

162



163

164 **Fig. 1. Schematic of the experimental design.** Line color and shape refers to the pCO₂ treatments
165 during the initial 110-day acclimation period (blue triangles, ambient pCO₂; red circles, elevated
166 pCO₂). Shading is in reference to the secondary exposure conditions (light, ambient pCO₂;
167 medium, moderate pCO₂; dark, severe pCO₂). Tertiary exposure conditions, following a 7-day
168 ambient recovery period, are indicated by shape and line type (empty and solid, ambient pCO₂;
169 filled and dashed, moderate pCO₂). Points indicate sampling days for respiration and shell growth
170 measurements and fixed tissues.

171

172 2.3 Modified reciprocal exposure

173 Secondary Exposure:

174 To begin the secondary exposure, juvenile geoducks (~2,200 geoduck initial pCO₂
175 treatment⁻¹) were rinsed on a 3×10⁵ μm screen to isolate individuals and were divided equally in
176 36 175-ml plastic cups (N=120 animals cup⁻¹, N=6 cups treatment⁻¹) each with 50 ml rinsed sand
177 (450-550 μm grain size). Seawater flowed into 250-L head tanks at a rate of 0.6 L min⁻¹ and was
178 pumped using submersible pumps to randomly interspersed cups each with a 1 gallon hour⁻¹
179 pressure compensating dripper (Raindrip). Flow rates from dripper manifolds to replicate cups
180 averaged 0.012 liters minute⁻¹ (~8 cycles hour⁻¹ for 175-ml). Juveniles acclimated under ambient
181 and elevated pCO₂ conditions were subjected to a secondary exposure period (7 days; Fig. 1) in
182 three pCO₂ conditions: ambient (754 ± 15 μatm), moderate (2750 ± 31 μatm), and severe (4940 ±
183 45 μatm; Table 1).

184 Ambient Recovery:

185 After secondary exposure, pCO₂ addition to head tank seawater ceased and all cups
186 returned to ambient conditions (896 ± 11 μatm, Table 1) for 7 days (Fig. 1).

187 Tertiary Exposure:

188 Replicate cups from the secondary exposure were split ($N=72$ cups) for subsequent tertiary
189 exposure (7 days; Fig. 1) in two conditions: ambient ($967 \pm 9 \mu\text{atm}$) and moderate $p\text{CO}_2$ ($3030 \pm$
190 $23 \mu\text{atm}$; Table 1).

191 Animals were randomly chosen for respiration and growth measurements as described
192 below ($N=3$ geoduck cup⁻¹) and fixed in liquid nitrogen ($N=6$ geoduck cup⁻¹) every three days and
193 at the start of every treatment transition, cumulatively as days 1, 4, 7 (secondary $p\text{CO}_2$ exposure),
194 8, 11, 14 (ambient recovery), 15, 18, and 21 (tertiary $p\text{CO}_2$ exposure; Fig. 1). Geoduck were fed
195 *ad libitum* a live mixed-algae diet of *Isocrysis*, *Tetraselmis*, *Chaetoceros*, and *Nano* throughout
196 the experiment ($4\text{-}5 \times 10^4$ cells ml⁻¹). Live algae cells were flowed into head tanks during the 21-
197 day modified reciprocal exposure at a semi-continuous rate (2.0×10^3 ml hr⁻¹ tank⁻¹) with a
198 programmable dosing pump (Jebao DP-4) to target 5×10^4 live algae cells ml⁻¹ in the 175-ml cups.
199 Large algae batch cultures were counted daily via bright-field image-based analysis (Nexcelom
200 T4 Cellometer; (Gurr et al., 2018) to calculate cell density of 2.5×10^4 live algae cells ml⁻¹ in the
201 250-L head tanks; the closed-bottom cups retained algae to roughly twice the head tank density
202 and algal density was analyzed in three cups via bright field image-based analysis every four days.

203 **2.4 Seawater chemistry**

204 Elevated $p\text{CO}_2$ levels in head tanks were controlled with a pH-stat system (Neptune Apex
205 Controller System; Putnam et al., 2016) and gas solenoid valves for a target pH of 7.2 for the
206 elevated and moderate $p\text{CO}_2$ condition and pH of 6.8 for the severe $p\text{CO}_2$ condition (pH in NBS
207 scale). pH and temperature (°C) were measured every 10 seconds by logger probes (Neptune
208 Systems; accuracy: ± 0.01 pH units and ± 0.1 °C, resolution: ± 0.1 pH units and ± 0.1 °C) positioned
209 in header tanks and trays.

210 Total alkalinity (TA; $\mu\text{mol kg}^{-1}$ seawater) of head tank, tray, and cup seawater was sampled
211 in combination with pH (total scale) by handheld probe (Mettler Toledo pH probe; resolution: 1
212 mV, 0.01 pH; accuracy: ± 1 mV, ± 0.01 pH; Thermo Scientific Orion Star A series A325), salinity
213 (Orion 013010MD Conductivity Cell; range 1 $\mu\text{S/cm}$ - 200 mS/cm; accuracy: ± 0.01 psu), and
214 temperature (Fisherbrand Traceable Platinum Ultra-Accurate Digital Thermometer; resolution;
215 0.001°C; accuracy: ± 0.05 °C). Quality control for pH data was assessed on each day with Tris
216 standard (Dickson Lab Tris Standard Batch T27). Carbonate chemistry was recorded weekly for
217 each replicate tray during the 110-day acclimation period and daily during the 21-day experiment

218 for three randomized cups representative of each $p\text{CO}_2$ treatment (days 1-7 and 8-15 $N=9$ cups;
219 days 15-21 $N=6$ cups). Additionally, carbonate chemistry of all cups was measured once weekly
220 during each 7-day period (days 1-7 and 8-15, $N=32$ cups; days 15-21, $N=72$ cups). TA was
221 measured using an open-cell titration (SOP 3b; Dickson et al., 2007) with certified HCl titrant
222 ($\sim 0.1 \text{ mol kg}^{-1}$, $\sim 0.6 \text{ mol kg}^{-1}$ NaCl; Dickson Lab, Batches A15 and A16) and TA measurements
223 identified $<1\%$ error when compared against certified reference materials (Dickson Lab CO_2 CRM
224 Batch 180). Seawater chemistry was completed following Guide to Best Practices (Dickson et al.
225 2007); TA and pH measurements were used to calculate carbonate chemistry, CO_2 , $p\text{CO}_2$, HCO_3^- ,
226 CO_3 , and Ω_{arag} , using the SEACARB package (Gattuso et al., 2018) in R v3.5.1 (R Core Team,
227 2018).

228 **2.5 Respiration rate and shell growth**

229 Respiration rates (oxygen consumption per unit time) were estimated by monitoring
230 oxygen concentration over time using calibrated optical sensor vials (PreSens, SensorVial SV-
231 PSt5-4ml) on a 24-well plate sensor system (Presens SDR SensorDish). Vials contained three
232 individuals per cup filled with $0.2 \mu\text{m}$ -filtered seawater from the corresponding treatment head
233 tank. Oxygen consumption from microbial activity was accounted for by including 5-6 vials filled
234 only with $0.2 \mu\text{m}$ -filtered treatment seawater. Respiration rates were measured in an incubator set
235 at 17°C , with the vials and plate sensor system fixed on a rotator for mixing. Oxygen concentration
236 ($\mu\text{g O}_2 \text{ L}^{-1}$) was recorded every 15 seconds until concentrations declined to $\sim 50\text{-}70\%$ saturation
237 (~ 20 minutes). Vial seawater volume was measured and clams from each vial were photographed
238 with a size standard (1 mm stage micrometer) to measure shell length (parallel to hinge; mm) using
239 Image J. Respiration rates were calculated using the R package LoLinR with suggested parameters
240 by the package authors (Olito et al., 2017) and following Gurr et al. (2020) with minor adjustments:
241 fixed constants for weighting method ($L\%$) and observations ($\alpha = 0.4$) over the full 20-minute
242 record. Final respiration rates of juvenile geoduck were corrected for blank vial rates and vial
243 seawater volume ($\mu\text{g O}_2 \text{ hr}^{-1} \text{ individual}^{-1}$).

244 **2.6 Physiological Assays**

245 Total antioxidant capacity (TAOC), total protein, and ash free dry weight (AFDW; organic
246 biomass) was measured for one animal from each biological tank replicate ($N=6$ animals treatment
247 1) at the end of secondary exposure (36 total animals) and at the end of tertiary exposure (72 total
248 animals). Whole animals were homogenized (Pro Scientific) with $300\text{-}500 \mu\text{l}$ cold $1\times\text{PBS}$ and total

249 homogenized volume (μl) was recorded. Homogenates were aliquoted for TAOC and total protein
250 assays and the remaining homogenate was used to measure organic biomass. TAOC was measured
251 in duplicate as the reduction capacity of copper reducing equivalents (CRE) following the
252 OxiselectTM microplate protocol (STA-360) and standardized to the total protein content of the
253 tissue lysate samples of the same individual ($\mu\text{M CRE mg protein}^{-1}$). Sample aliquots for total
254 protein were solubilized by adding 10 μl 1 M NaOH preceding incubation at 50°C and 800 RPM
255 for 4 hours and neutralized with 0.1 M HCl (pH 7). Total protein of tissue lysate samples was
256 measured using the Pierce Rapid Gold assay with bovine serum albumin following the PierceTM
257 microplate protocol (A53225). Total protein (mg) was standardized to organic biomass (mg protein
258 mg AFDW) following ignition (4.5 hours at 450°C) subtracted by the dry weight (24 hrs at 75°C)
259 and corrected for total homogenate volume.

260 **2.7 Statistical Analysis**

261 Welch's t-tests for unequal variances were used to analyze the effect of the initial 110-day
262 $p\text{CO}_2$ acclimation (fixed) on respiration rate and shell length prior to the 21-day exposure period.
263 A three-way analysis of variance (ANOVA) was used to analyze the effect of time (fixed) and
264 initial and secondary $p\text{CO}_2$ exposures (fixed) on respiration rate and shell growth for both the
265 secondary exposure and ambient recovery periods (days 1-7 and 8-14, respectively). A four-way
266 ANOVA was used to analyze the effect of time (fixed) and initial, secondary, and tertiary $p\text{CO}_2$
267 exposures (fixed) on respiration rate and shell growth during the tertiary exposure period (days 15-
268 21). Total antioxidant capacity, total protein, and organic biomass from samples on day 7 and day
269 21 were analyzed for effects of $p\text{CO}_2$ treatments (fixed) with two-way and three-way ANOVAs,
270 respectively. In all cases, normality assumptions were tested with visual inspection of diagnostic
271 plots (residual vs. fitted and normal Q-Q; (Kozak and Piepho, 2018) and homogeneity of variance
272 was tested with Levene's test (Brown and Forsythe, 1974). A pairwise Tukey's *a posteriori*
273 Honestly Significant Difference test was applied to significant model effects. All data analysis was
274 completed using R (v3.5.1; R Core Team, 2018).

275

276 **3. Results**

277 **3.1 Initial stress acclimation and secondary exposure to hypercapnic seawater**

278 There was no difference in respiration rate after 110 days of $p\text{CO}_2$ acclimation (Table 2;
279 Welch's t-test; initial, $t=-0.602$, $df=31.725$, $P=0.5516$), however the shell length of geoduck under

280 elevated $p\text{CO}_2$ was significantly larger, by 2.6%, compared to those under ambient treatment
 281 (Table 2; Welch's t-test; initial, $t=-4.297$, $df=2884$, $P<0.0001$). Under subsequent secondary
 282 exposure, the initial stress acclimation had a marginal effect on respiration rate (three-way
 283 ANOVA; initial, $F_{1,89}=3.409$, $P=0.068$) with 12.4% greater respiration rates in animals under
 284 elevated $p\text{CO}_2$ compared to animals under ambient conditions (Table 2). This effect was primarily
 285 driven by a marginal interaction effect under secondary $p\text{CO}_2$ treatment (three-way ANOVA;
 286 initial \times secondary, $F_{2,89}= 2.824$, $P=0.0647$), with 31% greater respiration rates under moderate
 287 $p\text{CO}_2$ stress in animals acclimated under elevated $p\text{CO}_2$ (Fig. 2a). Shell length increased
 288 significantly with time (three-way ANOVA; time, $F_{2,306}= 3.347$, $P=0.0365$; Tukey HSD, day 7 >
 289 day 4, $P=0.0236$) and independent of $p\text{CO}_2$ treatments (Table 2). Juvenile clams acclimated under
 290 elevated $p\text{CO}_2$ on average had significantly greater organic biomass (two-way ANOVA; initial,
 291 $F_{1,30}=9.313$, $P=0.0047$) at the end of the secondary exposure period (day 7) with 39% greater mg
 292 tissue AFDW individual⁻¹ compared to animals reared under ambient conditions (Table 3 and Fig,
 293 3c). There was no significant effect from initial or secondary $p\text{CO}_2$ treatments on total protein or
 294 TAOC (Table 3 and Figs. 3a and 3b).

295

296 **Table 2. Effects of $p\text{CO}_2$ stress exposures on mean respiration rate and shell growth of**
 297 ***Panopea generosa*.** A Welch's t-test tested for effects of $p\text{CO}_2$ stress acclimation prior to the 21-
 298 day experiment. Three-way and four-way ANOVA tests were used under the secondary and
 299 tertiary exposure periods and a three-way ANOVA tested for treatment effects during the ambient
 300 recovery period. Significant effects are bolded for $P < 0.05$.

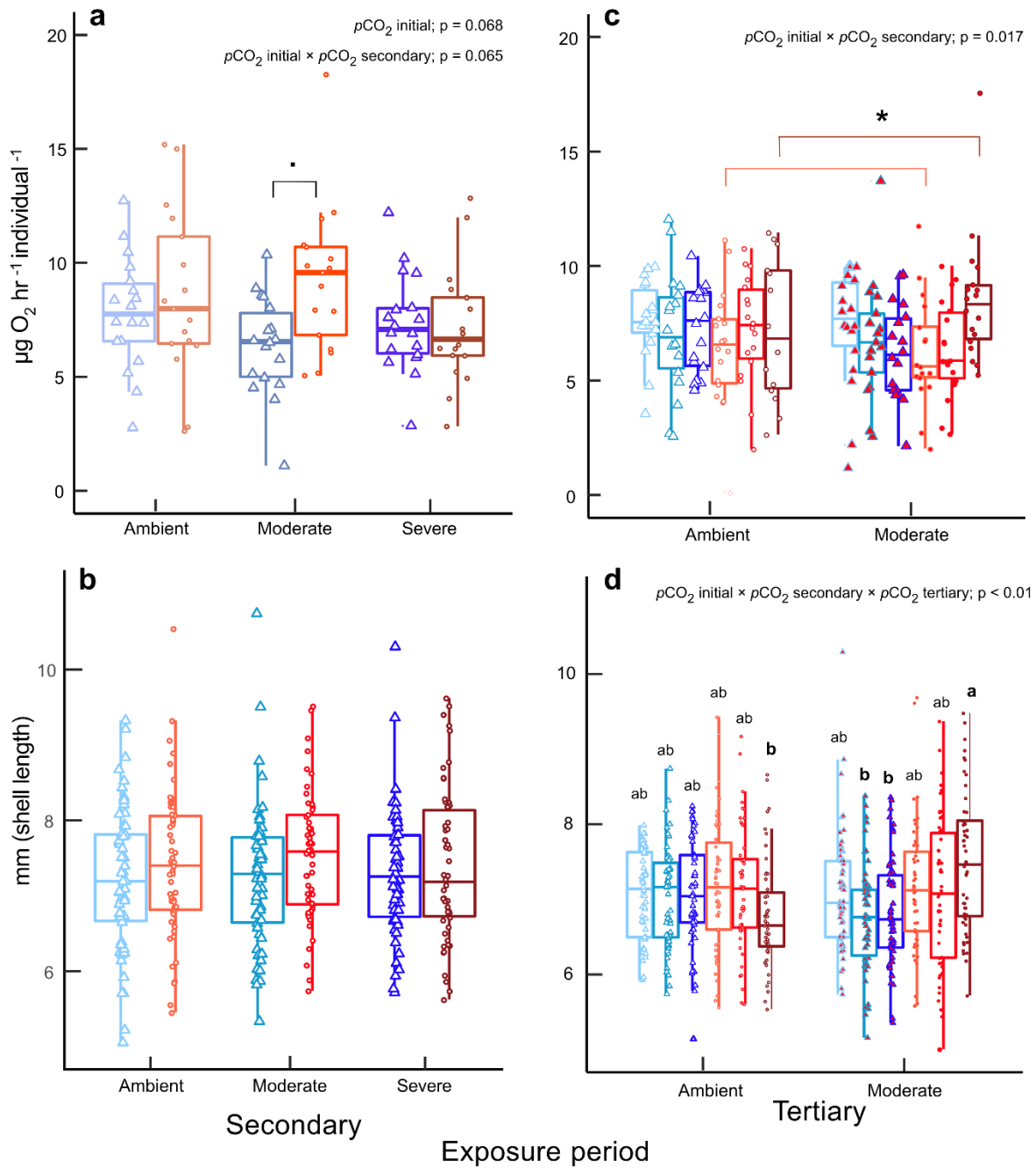
Effect	Respiration rate			Shell length		
	<i>df</i>	<i>F</i>	<i>P</i>	<i>df</i>	<i>F</i>	<i>P</i>
Pre-experiment	<i>t-test</i>					
$p\text{CO}_2$ initial	31.725	-	0.5516	2884	-	<0.0001
Days 1-7	<i>Three-way ANOVA</i>					
$p\text{CO}_2$ initial	1,89	3.409	<i>0.0681</i>	1,306	3.442	<i>0.0645</i>
$p\text{CO}_2$ secondary	2,89	0.584	0.5596	2,306	0.137	0.8722
time	2,89	1.450	0.2400	2,306	3.447	0.0331
$p\text{CO}_2$ initial \times $p\text{CO}_2$ secondary	2,89	2.824	0.0647	2,306	0.235	0.7909
$p\text{CO}_2$ initial \times time	2,89	1.155	0.3199	2,306	0.018	0.9822
$p\text{CO}_2$ secondary \times time	4,89	1.486	0.2131	4,306	0.145	0.9650
$p\text{CO}_2$ initial \times $p\text{CO}_2$ secondary \times time	4,89	0.573	0.6830	4,306	1.2870	0.2749
Days 8-14	<i>Three-way ANOVA</i>					
$p\text{CO}_2$ initial	1,87	0.149	0.7007	1,306	1.652	0.1995

$p\text{CO}_2$ secondary	2,87	2.328	0.1035		2,306	0.647	0.5242
time	2,87	3.719	0.0282		2,306	6.673	0.0015
$p\text{CO}_2$ initial \times $p\text{CO}_2$ secondary	2,87	1.004	0.3707		2,306	0.051	0.95
$p\text{CO}_2$ initial \times time	2,87	1.127	0.3288		2,306	0.542	0.5821
$p\text{CO}_2$ secondary \times time	4,87	1.325	0.2672		4,306	0.824	0.5105
$p\text{CO}_2$ initial \times $p\text{CO}_2$ secondary \times time	4,87	0.597	0.6657		4,306	0.353	0.8417
Days 15-21	<i>Four-way ANOVA</i>						
$p\text{CO}_2$ initial	1,174	0.022	0.8800		1,606	8.421	0.0038
$p\text{CO}_2$ secondary	2,174	0.726	0.4583		2,606	1.172	0.3104
$p\text{CO}_2$ tertiary	1,174	0.556	0.4570		1,606	0.199	0.6560
time	1,174	0.088	0.9157		2,606	21.638	<0.0001
$p\text{CO}_2$ initial \times $p\text{CO}_2$ secondary	2,174	4.149	0.0174		2,606	0.423	0.6556
$p\text{CO}_2$ initial \times $p\text{CO}_2$ tertiary	1,174	0.747	0.3888		1,606	8.195	0.0044
$p\text{CO}_2$ secondary \times $p\text{CO}_2$ tertiary	2,174	0.339	0.7131		2,606	3.775	0.0235
$p\text{CO}_2$ initial \times time	2,174	0.051	0.9502		2,606	1.001	0.3683
$p\text{CO}_2$ secondary \times time	4,174	1.212	0.3077		4,606	1.393	0.2350
$p\text{CO}_2$ tertiary \times time	2,174	0.023	0.9772		2,606	0.329	0.7199
$p\text{CO}_2$ initial \times $p\text{CO}_2$ secondary \times $p\text{CO}_2$ tertiary	2,174	1.812	0.1664		2,606	6.352	0.0019
$p\text{CO}_2$ initial \times $p\text{CO}_2$ secondary \times time	4,174	1.689	0.1545		4,606	1.244	0.2910
$p\text{CO}_2$ initial \times $p\text{CO}_2$ tertiary \times time	2,174	1.139	0.3227		2,606	0.301	0.7404
$p\text{CO}_2$ secondary \times $p\text{CO}_2$ tertiary \times time	4,174	1.396	0.2373		4,606	0.770	0.5452
$p\text{CO}_2$ initial \times $p\text{CO}_2$ secondary \times $p\text{CO}_2$ tertiary \times time	4,174	0.577	0.6798		4,606	0.499	0.7367
Significant P-values (< 0.05) are bolded; marginal P-values (<0.1) in <i>italics</i>							

301

302 **Table 3. Effects of $p\text{CO}_2$ stress exposures on antioxidant capacity, total protein, and**
 303 **organic biomass (AFDW) of *Panopea generosa*.** Two-way and three-way ANOVA tests for
 304 differences in physiological and cellular status on days 7 and 21 of the 21-day exposure period,
 305 respectively. Significant effects are bolded for $P < 0.05$.

Effect	Antioxidant capacity			Total protein			AFDW		
	<i>df</i>	<i>F</i>	<i>P</i>	<i>df</i>	<i>F</i>	<i>P</i>	<i>df</i>	<i>F</i>	<i>P</i>
DAY 7	<i>Two-way ANOVA</i>								
$p\text{CO}_2$ initial	1,30	0.005	0.942	1,30	0.003	0.959	1,30	9.313	0.0047
$p\text{CO}_2$ secondary	2,30	0.143	0.867	2,30	0.866	0.431	2,30	2.536	0.096
$p\text{CO}_2$ initial \times $p\text{CO}_2$ secondary	2,30	1.007	0.377	2,30	2.136	0.136	2,30	0.158	0.8546
DAY 21	<i>Three-way ANOVA</i>								
$p\text{CO}_2$ initial	1,56	8.069	0.0063	1,56	2.365	0.13	1,56	12.899	<0.001
$p\text{CO}_2$ secondary	2,56	0.164	0.849	2,56	0.625	0.539	2,56	1.578	0.2153
$p\text{CO}_2$ tertiary	1,56	2.161	0.1471	1,56	1.272	0.264	1,56	3.298	<i>0.0747</i>
$p\text{CO}_2$ initial \times $p\text{CO}_2$ secondary	2,56	1.43	0.248	2,56	1.423	0.25	2,56	1.756	0.1822
$p\text{CO}_2$ initial \times $p\text{CO}_2$ tertiary	1,56	0.678	0.4136	1,56	2.25	0.139	1,56	0.453	0.5036
$p\text{CO}_2$ secondary \times $p\text{CO}_2$ tertiary	2,56	0.752	0.476	2,56	0.225	0.8	2,56	0.166	0.8906
$p\text{CO}_2$ initial \times $p\text{CO}_2$ secondary \times $p\text{CO}_2$ tertiary	2,56	0.141	0.8688	2,56	0.26	0.772	2,56	0.181	0.8353
Significant P-values (< 0.05) are bolded; marginal P-values (<0.1) in <i>italics</i>									



306

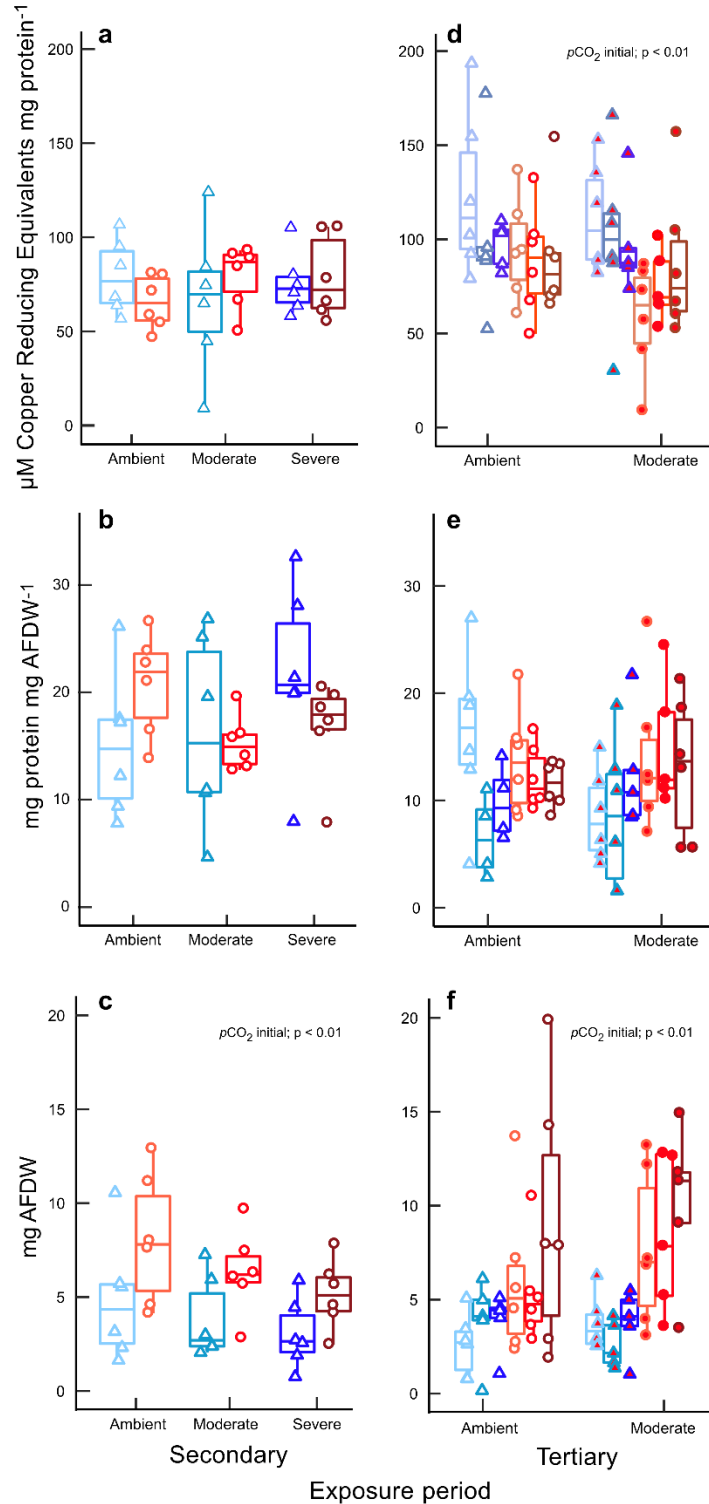
307 **Fig. 2. Respiration rate and shell length under secondary (a and b) and tertiary (c and d)**

308 **exposure periods.** Color, shapes, and fill are in reference to Figure 1. Significant *a posteriori*

309 effects are shown as letters or an asterisk.

310

311



312

313 **Fig. 3. Antioxidant response and physiology of fixed animals at the end of secondary (a-c;**

314 **day 14) and tertiary treatments (d-f; day 21). Color, shapes, and fill are in reference to Figure**

315 1.

316 **3.2 Ambient common garden recovery under normocapnic conditions**

317 During ambient recovery, respiration rate was not significantly affected by initial or
318 secondary $p\text{CO}_2$ treatments, but was significantly affected by time (Table 2; three-way ANOVA;
319 time, $F_{2,87}=3.719$, $P=0.0282$) with an increase in respiration rates over the 7-day period (Tukey
320 HSD; day 14 > day 8; $P = 0.0254$). Similarly, shell growth was not significantly affected by initial
321 or secondary $p\text{CO}_2$ treatment, but showed a significant increase with time (Table 2; three-way
322 ANOVA; time, $F_{2,306}=6.643$, $P=0.0015$; Tukey HSD; day 14 > day 8, $P=0.013$; Tukey HSD, day
323 11 > day 8, $P=0.001$).

324 **3.3 Tertiary exposure to hypercapnic seawater**

325 The interaction of initial and secondary $p\text{CO}_2$ treatments had a significant effect on
326 respiration rate under tertiary exposure (Table 2; four-way ANOVA; initial \times secondary, $F_{2,174}=$
327 4.149, $P=0.0174$), with this interaction primarily driven by a 20.4% greater respiration rate in $p\text{CO}_2$
328 stress-acclimated animals exposed to severe and ambient $p\text{CO}_2$ during the secondary period (Fig.
329 2c), although the post-hoc test was only marginally significant (Tukey HSD; moderate \times severe >
330 moderate \times ambient, $P=0.0685$). Shell growth was affected by an interaction between initial,
331 secondary, and tertiary $p\text{CO}_2$ treatments (Table 2 and Fig. 2d; four-way ANOVA;
332 initial \times secondary \times tertiary, $F_{2,606}=6.352$, $P=0.0019$). Pairwise differences of the three-way
333 treatment interaction showed 9.3% greater mean shell size by acclimated animals with secondary
334 and tertiary exposure to severe and moderate $p\text{CO}_2$, respectively (Fig. 2d). At the end of the tertiary
335 exposure period (day 21), initial stress acclimation under elevated $p\text{CO}_2$ increased organic biomass
336 (Table 3; three-way ANOVA; initial, $F_{1,56}=12.899$, $P<0.001$) and tertiary exposure had a marginal
337 increase (three-way ANOVA; tertiary, $F_{1,56}=3.298$, $P=0.0604$) with 51% and 28% greater organic
338 biomass under stress treatments relative to ambient controls (Fig. 3f). There was a significant effect
339 of initial stress acclimation on antioxidant activity (Table 3; three-way ANOVA; initial,
340 $F_{1,56}=8.069$, $P=0.0063$) with 22% greater $\mu\text{M CRE mg protein}^{-1}$ by clams reared under ambient
341 $p\text{CO}_2$ (Fig. 3d); there was no effect of $p\text{CO}_2$ treatment or two-way and three-way interactions of
342 $p\text{CO}_2$ treatments on total protein (Table 3 and Fig. 3e).

343

344 **4. Discussion**

345 In the present study we evaluated the effects of postlarval stress acclimation and subsequent
346 exposures to elevated $p\text{CO}_2$ on the physiological and oxidative stress response in juvenile geoduck.

347 Our findings suggest moderate hypercapnic conditions during postlarval development improves
348 metrics of physiological performance and CSR. This novel investigation of adaptive stress
349 acclimation demonstrates a high tolerance to $p\text{CO}_2$ regimes ($\sim 2500\text{-}5000 \mu\text{atm}$) and plasticity of
350 bioenergetic and subcellular responses beneficial for later performance in *Panopea generosa*.

351 **4.1 Stress-intensity- and life-stage-dependent effects**

352 Survival under long-term stress exposure and positive physiological responses of
353 acclimated animals under ‘moderate’ ($\sim 2900 \mu\text{atm } p\text{CO}_2$ 0.4Ω) and ‘severe’ ($\sim 4800 \mu\text{atm } p\text{CO}_2$
354 0.2Ω) reciprocal exposures highlights the resilience of *Panopea generosa* to OA and suggests that
355 stress acclimation (days) can induce beneficial effects during postlarval-juvenile development.
356 Specifically, clams repeatedly exposed to the greatest intensity of stress
357 (moderate \times severe \times moderate) had both greater respiration rates and shell size (Table 2; Fig. 2).
358 Further, stress-acclimated individuals had greater organic biomass and lower amounts of
359 antioxidant proteins relative to ambient controls (Figs. 3c, 3d, and 3f), suggesting optimized tissue
360 accretion and energy partitioning, coupled with decreased costs for cytoprotection. Previous
361 studies describe metabolic compensation and regulation of CSR during hypercapnia as attributes
362 of a well-adapted stress response to control acid-base status and normal
363 development/metamorphosis (Walsh and Louise Milligan, 1989; Dineshram et al., 2015). Indeed,
364 prior work on juvenile *P. generosa* also demonstrates positive acclimatory carryover effects, with
365 increased shell length and metabolic rate after repeat exposures to hypercapnic and undersaturated
366 conditions with respect to aragonite (Gurr et al., 2020). Contrary to these findings, similar $p\text{CO}_2$
367 and Ω levels decrease metabolic rate and scope for growth in the mussel *Mytilus chilensis* (Navarro
368 et al., 2013), cause a three-fold increase in mortality rate in juvenile hard clam *Mercenaria*
369 *mercenaria* (Green et al., 2009), and alter metamorphosis and juvenile burrowing behavior in
370 *Panopea japonica* (Huo et al., 2019). Thus, $p\text{CO}_2$ tolerance limitations are likely species-specific,
371 as well as life stage, duration, and stress-intensity specific.

372 $p\text{CO}_2$ -induced phenotypic variation over postlarval-juvenile development observed in this
373 study suggests postlarval stages may be optimal for stress acclimation. Beneficial carryover effects
374 herein are also corroborated with compensatory physiology and differential DNA methylation of
375 juvenile *P. generosa* in other studies (Putnam et al., 2017; Gurr et al., 2020). In contrast, OA can
376 have deleterious effects on growth/development, settlement, and proteomic composition of larval
377 *P. generosa* (Timmins-Schiffman et al., 2020), further emphasizing life-stage dependence of $p\text{CO}_2$

378 stress exposure. Mollusc larvae are widely established to have enhanced susceptibility to OA with
379 impacts on shell growth and developmental transition (Kurihara et al., 2007; Kapsenberg et al.,
380 2018). For example, larval exposure to elevated $p\text{CO}_2$ leads to persistent negative effects (i.e.
381 reduced shell growth and development) in Pacific oyster *Crassostreas gigas*, Olympia oyster
382 *Ostrea lurida*, and bay scallop *Argopecten irradians* (Barton et al., 2012; Hettinger et al., 2012;
383 White et al., 2013). Beneficial responses to OA are also possible, especially in longer term and
384 carryover-effect studies (Parker et al., 2015). For example, elevated $p\text{CO}_2$ during gametogenesis
385 in the Chilean mussel *Mytilus chilensis* and Sydney rock oyster *Saccostrea glomerata* increases
386 the size of larval stages in progeny (Parker et al., 2012; Diaz et al., 2018). Future comparative
387 studies should test stress responses of well-defined inter- and subtidal molluscs to determine if
388 pre-conceived tolerance limitations are affected by repeated dose-responses post-settlement.

389 Our observation of beneficial effects in stress-acclimated clams suggest an adaptive
390 resilience of *P. generosa* to hypercapnic conditions relevant to postlarval-juvenile development in
391 both natural and aquaculture systems. *P. generosa* are likely capable of adaptive resilience
392 particularly during this life stage because $p\text{CO}_2$ and Ω gradients naturally occur alongside the
393 dramatic developmental transition from free-swimming larvae to sessile benthic juveniles. Habitat
394 within the native range of *P. generosa* exhibits elevated $p\text{CO}_2$ and aragonite undersaturation with
395 episodic/seasonal variation (surface water $\Omega < 1$ in winter months, Dabob Bay in Hood Canal, WA;
396 Fassbender et al., 2018) and geographical ($> 2400 \mu\text{atm}$ and $\Omega < 0.4$ in Hood Canal, WA; Feely et
397 al., 2010) and vertical heterogeneity (Reum et al., 2014) comparable to gradients within sub-
398 surface sediments (Ω 0.4-0.6; Green et al., 2009). Meseck et al. (2018) found *in-situ* porewater pH
399 increases model predictability of bivalve community composition, *Mya arenaria* and *Nucula* spp,
400 suggesting sediment acidification and carbonate chemistry influence bivalve settlement. Our
401 experimental timing and findings overlaid on common geoduck aquaculture practices suggest
402 postlarval ‘settlement’ as an ecologically-relevant window to investigate the adaptive capacity for
403 stress acclimatization.

404 **4.2 Oxidative status and repeated stress encounters**

405 Our results herein demonstrate activation of phenotypic variation after repeated stress
406 encounters suggesting postlarval stress acclimation may have a critical role in subsequent stress
407 response. A growing body of research supporting conditioning-hormesis challenges the paradigm
408 of primarily deleterious effects of stress exposure (Calabrese et al., 2007; Costantini et al., 2012;

409 Gurr et al., 2020). Here we posit that hormetic priming could be occurring through moderate
410 oxidative stress on protein homeostasis (patterns of differential expression), cellular signaling, and
411 mitochondrially-mediated responses. For example, Constantini et al. (2012) found early-life
412 exposure of the zebra finch *Taeniopygia guttata* to thermal-induced oxidative damage decreased
413 oxidative stress under subsequent thermal exposure during adulthood. This low-dose stimulatory
414 effect of oxidative stress is well-characterized (i.e. under calorie restriction, hypoxia, and exercise;
415 Ristow and Schmeisser, 2014) for a wide range of taxa (Constantini et al., 2012; Visser et al., 2018;
416 Zhang et al., 2018), but remains poorly understood in response to OA conditions.

417 In *Panopea generosa* in this study, compensatory antioxidant synthesis reduced
418 performance in absence of prior stress acclimation suggesting an adaptive role of oxidative stress
419 and conditioning-hormesis. pH- and CO₂-induced oxidative stress and antioxidant response are of
420 growing interest to characterize stress resilience in bivalves (Tomanek et al., 2011; Matoo et al.,
421 2013). Oxidative stress is intensified by acidosis (low intracellular pH) and hypercapnia either
422 indirectly from low pH on ferrous iron enhancing the Fenton reaction (producing hydroxyl
423 radicals), or a direct interaction of intracellular hypercapnia on free radical formation (Tomanek
424 et al., 2011). pH- or CO₂-induced stress and mediative responses are species and stress-dependent
425 (i.e. frequency, duration, and magnitude of stress exposures). Under short and prolonged exposure
426 to subtle hypercapnic seawater (2-15 weeks; ~800 μatm, 7.9 pH, and 3 Ω), the Eastern oyster
427 *Crassostrea virginica* and hard clam *M. mercenaria* differ in initial antioxidant production
428 suggesting that CSR can determine interspecies vulnerability to hypercapnic seawater (Matoo et
429 al., 2013). In more pronounced hypercapnic and aragonite undersaturated conditions, *C. virginica*
430 upregulates antioxidant proteins (14 days; ~3500 μatm and 7.5 pH; Tomanek et al., 2011) and a
431 similar response is also seen in the Yesso scallop *Patinopecten yessoensis* (duration = 14 days;
432 ~2200 μatm, 7.5 pH, and 0.7 Ω; Liao et al., 2019) and mussel *Mytilus coruscus* (duration = 45
433 days; ~2800 μatm, 7.3 pH, and 0.5 Ω; Huang et al., 2018). Alternatively, a seemingly ‘preparatory’
434 energetic cost of antioxidant synthesis is found in a variety of taxa (Hermes-Lima and Zenteno-
435 Savín, 2002; Ivanina and Sokolova, 2016) and suggests adaptive energy reallocation to scavenge
436 ROS formed by aerobic recovery when a stressor is lifted.

437 Intermittent oxidative stress may have evolutionary importance in stress resilience of long-
438 lived marine bivalves. The ocean quahog *Arctica islandica* is the oldest known non-colonial
439 animal; their substantial longevity is hypothesized to be driven by intermittent metabolic-

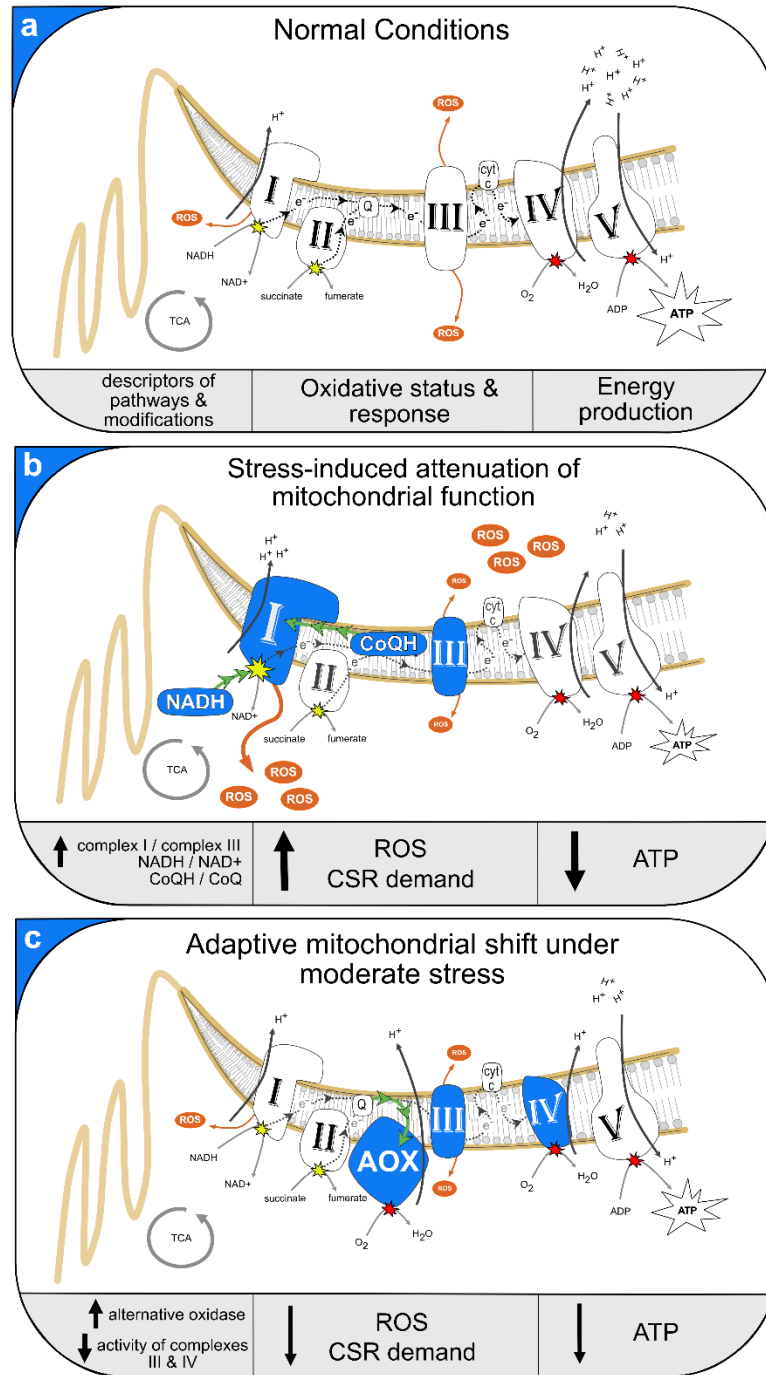
440 quiescence (dormancy when burrowed) demanding resilience to ROS overproduction (oxidative
441 bursts) and resistance to cell death upon subsequent aerobic-recovery (Abele et al., 2008).
442 Interestingly, *A. islandica* have a particularly low peroxidation-sensitive lipids (Munro and Blier,
443 2012) and high baseline antioxidant capacity throughout their lifespan suggesting an adaptive
444 resilience to oxidative damage (Abele et al., 2008). Whereas intertidal molluscs (i.e. *Mytilus sp.*,
445 *Crassostrea sp.*, and *Argopecten sp.*) have energetic deficits under dynamic environmental stress
446 (i.e. elevated metabolic demand, ROS production, and antioxidant response; Kelley et al., 2017;
447 Liao et al., 2019), *A. islandica* continues ventilation without anaerobic transition or overproduction
448 of free radicals (Strahl et al., 2011). Thus, lower antioxidant production by stress-conditioned *P.*
449 *generosa* could suggest adaptive subcellular mechanism(s) common across long-lived bivalves to
450 maintain redox status under frequent or intermittent stress exposures. Altogether, the contrasting
451 response of lower antioxidant proteins in stress-acclimated *P. generosa* suggests beneficial effects
452 of prior exposure to hypercapnic seawater, which highlights the need for a mechanistic
453 understanding of the role of oxidative stress in this process.

454 **4.3 Mitochondrial and molecular mechanisms of moderate stress acclimation**

455 Based on the effects of stress acclimation on antioxidant capacity and performance of
456 *Panopea generosa* in this study, we describe two possible subcellular mechanisms underpinning
457 stress-intensity-dependent effects on mitochondrial pathways and energy partitioning: 1) stress-
458 induced attenuation of mitochondrial function and 2) adaptive mitochondrial shift under moderate
459 stress (Fig. 4).

460 1) Stress-induced attenuation of mitochondrial function: Individuals initially exposed to
461 ambient $p\text{CO}_2$ increased antioxidant proteins and decreased growth relative to stress-acclimated
462 clams suggesting a greater demand for CSR leading to negative performance. Hypercapnia and
463 acidosis can directly and indirectly drive increased formation of free radicals (Murphy, 2009;
464 Tomanek et al., 2011) and elicit changes in the activity (Lambert and Brand, 2004) and expression
465 of mitochondrial complexes (Dineshram et al., 2012; Dineshram et al., 2015), which altogether
466 suggests diminished mitochondrial ATPs under environmental stress (Murphy 2009). Under
467 normal aerobic respiration (Fig. 4a), complexes I (NADH dehydrogenase) and III (cytochrome *c*
468 oxidoreductase) are dominant sources of mitochondrial ROS production by the electron transport
469 chain (mETC). In contrast, mitochondrial dysfunction or alterations of mETC occur under
470 environmental stress in which high pools of NADH in the mitochondrial matrix and reduced

471 coenzyme Q shift electron transport (reverse electron transport or RET) and proton gradient control
472 to complex I, eliciting a deficit for ATPs and enhanced ROS production and CSR demand
473 (Murphy, 2009); Fig 4b). Further, increased protonmotive force and pH gradient of the inner
474 mitochondrial membrane increases RET and ROS production (Lambert and Brand, 2004; Miwa
475 and Brand, 2003) suggesting a mechanism of pH- and CO₂-induced mitochondrial dysfunction.
476 Altogether, the upregulation of antioxidant proteins and reduced growth in unconditioned *P.*
477 *generosa* are likely outcomes of acclimation-dependent attenuation of mitochondrial function (Fig.
478 4b). In addition, uncoupling proteins (UCPs) are activated under oxidative damage to mediate
479 mitochondrial stress although further decreasing the proton gradient and ATP production
480 (Slocinska et al., 2016).



481

482 **Fig. 4. Hypothesized model of stress acclimation through mitochondrial pathways:** Diagram
 483 of inner mitochondrial membrane under normal conditions (a), dysfunction (b; i.e. reverse
 484 electrician transport), and the AOX pathway (c). Solid blue shapes highlight descriptors of
 485 modified pathways and green arrows display shifts in the direction of electrons (b and c). Legends
 486 with solid black arrows display the direction of changes relative to the mETC under normal
 487 conditions.

488 2) Adaptive mitochondrial shift under moderate stress: Alternative oxidase (AOX) is a
489 regulatory protein of the inner mitochondrial membrane that receives electrons from ubiquinol to
490 reduce oxygen and produce ATP without involving the cytochrome *c* mETC pathway (Figs. 4a
491 and 4c). There is growing interest in AOX as a compensatory response that permits ATP synthesis
492 and reduces ROS production during stress exposure (Tschischka et al., 2000; Sussarellu et al.,
493 2013; Yusseppone et al., 2018). Although previously theorized as an exclusive mechanism in plant
494 mitochondria (Vanlerberghe, 2013), molecular tools have helped define an evolutionary
495 diversification of AOX in higher order animalia (McDonald and Vanlerberghe, 2006) with a
496 particular prevalence in marine invertebrates and bivalve genomes (McDonald et al., 2009). AOX
497 permits oxidative phosphorylation when complexes III and IV are inhibited (i.e. cyanide and
498 sulphide inhibition), or when ROS is overproduced. A pH decline within the inner mitochondrial
499 membrane can also activate the AOX pathway (Lima-Júnior et al., 2000). Although less efficient,
500 with one-third of the membrane potential relative to cytochrome *c* mETC pathway (Millenaar and
501 Lambers, 2003), AOX activity protects against free radical formation under abiotic and biotic
502 disturbances (McDonald et al., 2009). Upregulated AOX coupled with decreased antioxidant
503 protein synthesis under thermal stress suggests regulatory control of redox status, cellular
504 signaling, and downstream energy allocation (Maxwell et al., 1999) are possible using this
505 pathway. For example, *C. gigas* upregulates AOX in response to hypoxia-reoxygenation
506 suggesting anticipatory dissipation of the proton gradient to avoid overproduction of free radicals
507 upon reoxygenation (Sussarellu et al., 2013). An AOX-mediated response corroborates our
508 hypothesis of a mechanism for hormesis that may outweigh energetic costs of the reduced ATP
509 efficiency from this AOX pathway. A BLAST search identified AOX, mitochondrial carrier
510 proteins (UCPs), and conserved mETC complexes within an annotated Pacific geoduck draft
511 genome (Roberts et al., 2020). qPCR and metabolomics are planned to investigate these proposed
512 mechanisms of hypercapnic-induced modification of mitochondrial function and link complexes I
513 and III, AOX, reduced cofactors, UCPs, and ATP under acute and repeated stress encounters.

514 **5. Conclusion**

515 Postlarval acclimation under moderate hypercapnia can elicit beneficial phenotypes under
516 subsequent stress encounters. This acclimatory capacity is likely contingent on stress-intensity (i.e.
517 magnitude, duration, frequency of stress periods) and timing during postlarval settlement and
518 juvenile development. Thus, investigations of marine species responses to climate change should

519 consider adaptive dose-dependent regulation and effects post-acclimation. Further, alternative
520 mitochondrial pathways can build an understanding of mechanisms underpinning hormesis to
521 provide additional ‘climate-proofing’ strategies in aquaculture and conservation of goods and
522 services in the Anthropocene.

523 **Acknowledgments**

524 We thank the Jamestown S’Klallam Tribe and Kurt Grinnell for providing the animals and
525 facilities for this research. We also thank management staff and technicians at the Jamestown Point
526 Whitney Shellfish Hatchery, Matt Henderson, Josh Valley and Clara Duncan, for their assistance.
527 We also thank Emma Strand for analytical support.

528

529 **Competing interests:**

530 The authors declare no competing or financial interests.

531

532 **Author contributions**

533 S.J.G., B.V., S.B.R. and H.M.P. designed the experiments, S.J.G. conducted the experiments and
534 analyzed data, S.J.G., S.A.T, B.V., S.B.R. and H.M.P. drafted, revised, read and approved the final
535 version of the manuscript for publication.

536

537 **Funding:**

538 This work was funded in part through a grant from the Foundation for Food and Agriculture
539 research; Grant ID: 554012, Development of Environmental Conditioning Practices to
540 Decrease Impacts of Climate Change on Shellfish Aquaculture. The content of this publication is
541 solely the responsibility of the authors and does not necessarily represent the official views of the
542 Foundation for Food and Agriculture Research. Analysis and research materials were also
543 supplemented by the Melbourne R. Carriker Student Research Grant.

544

545 **Data availability**

546 All raw data and statistical code are openly available as a Zenodo repository:
547 <http://doi.org/10.5281/zenodo.3903019> (Gurr et al. 2020).

548

549

550 **References**

551

552 **Abele, D., Strahl, J., Brey, T. and Philipp, E. E. R.** (2008). Imperceptible senescence: ageing in
553 the ocean quahog *Arctica islandica*. *Free Radic. Res.* **42**, 474–480.

554

555 **An, M. I. and Choi, C. Y.** (2010). Activity of antioxidant enzymes and physiological responses in
556 ark shell, *Scapharca broughtonii*, exposed to thermal and osmotic stress: effects on
557 hemolymph and biochemical parameters. *Comp. Biochem. Physiol. B Biochem. Mol. Biol.*
558 **155**, 34–42.

559

560 **Barton, A., Hales, B., Waldbusser, G. G., Langdon, C. and Feely, R. A.** (2012). The Pacific
561 oyster, *Crassostrea gigas*, shows negative correlation to naturally elevated carbon dioxide
562 levels: Implications for near-term ocean acidification effects. *Limnol. Oceanogr.* **57**, 698–710.

563

564 **Brown, B., Dunne, R., Goodson, M. and Douglas, A.** (2002). Experience shapes the
565 susceptibility of a reef coral to bleaching. *Coral Reefs* **21**, 119–126.

566

567 **Brown, M. B. and Forsythe, A. B.** (1974). Robust tests for the equality of variances. *J. A. Stat.*
568 *Assoc.* **69**, 364–367.

569

570 **Cai, W. J., Hu, X., Huang, W.-J., Murrell, M. C., Lehrter, J. C., Lohrenz, S. E., Chou, W.-C.,**
571 **Zhai, W., Hollibaugh, J. T., Wang, Y., et al.** (2011). Acidification of subsurface coastal
572 waters enhanced by eutrophication. *Nat. Geosci.* **4**, 766–770.

573

574 **Calabrese, E. J., Bachmann, K. A., Bailer, A. J., Bolger, P. M., Borak, J., Cai, L.,**
575 **Cedergreen, N., Cherian, M. G., Chiueh, C. C., Clarkson, T. W., et al.** (2007). Biological
576 stress response terminology: Integrating the concepts of adaptive response and
577 preconditioning stress within a hormetic dose-response framework. *Toxicol. Appl. Pharmacol.*
578 **222**, 122–128.

579

- 580 **Costantini, D.** (2014). Oxidative stress and hormesis in evolutionary ecology and physiology.
581 Springer-Verlag, Berlin and Heidelberg, Germany. 978-3-642-54663-1.
582
- 583 **Costantini, D., Monaghan, P. and Metcalfe, N. B.** (2012). Early life experience primes resistance
584 to oxidative stress. *J. Exp. Biol.* **215**, 2820–2826.
585
- 586 **Diaz, R., Lardies, M. A., Tapia, F. J., Tarifeño, E. and Vargas, C. A.** (2018). Transgenerational
587 effects of pCO₂-driven ocean acidification on adult mussels *Mytilus chilensis* modulate
588 physiological response to multiple stressors in larvae. *Front. Physiol.* **9**, 1349.
589
- 590 **Dickson, A. G., Sabine, C. L. and Christian, J. R. eds.** (2007). *Guide to Best Practices for*
591 *Ocean CO₂ Measurements*. PICES Special Publication 3: 191
592
- 593 **Dineshram, R., Wong, K. K. W., Xiao, S., Yu, Z., Qian, P. Y. and Thiyagarajan, V.** (2012).
594 Analysis of Pacific oyster larval proteome and its response to high-CO₂. *Mar. Pollut. Bull.*
595 **64**, 2160–2167.
596
- 597 **Dineshram, R., Quan, Q., Sharma, R., Chandramouli, K., Yalamanchili, H. K., Chu, I. and**
598 **Thiyagarajan, V.** (2015). Comparative and quantitative proteomics reveal the adaptive
599 strategies of oyster larvae to ocean acidification. *Proteomics* **15**, 4120–4134.
600
- 601 **Fassbender, A. J., Alin, S. R., Feely, R. A., Sutton, A. J., Newton, J. A., Krembs, C., Bos, J.,**
602 **Keyzers, M., Devol, A., Ruef, W., et al.** (2018). Seasonal carbonate chemistry variability in
603 marine surface waters of the US Pacific Northwest. *Earth Syst. Sci. Data* **10**, 1367–1401.
604
- 605 **Fawcett, T. W. and Frankenhuis, W. E.** (2015). Adaptive explanations for sensitive windows in
606 development. *Front. Zool.* **12 Suppl 1**, S3.
607
- 608 **Feely, R. A., Alin, S. R., Newton, J., Sabine, C. L., Warner, M., Devol, A., Krembs, C. and**
609 **Maloy, C.** (2010). The combined effects of ocean acidification, mixing, and respiration on pH
610 and carbonate saturation in an urbanized estuary. *Estuar. Coast. Shelf S.* **88**, 442–449.

611

612 **Gattuso, J. P., Epitalon, J. M. and Lavine, H.** (2018). Seacarb: Seawater Carbonate Chemistry.

613

614 **Goodwin, C. L. and Pease, B.** (1987). The distribution of geoduck (*Panope abrupta*) size, density,

615 and quality to habitat characteristics such as geographic area, water depth, sediment type, and

616 associated flora and fauna in Puget Sound, Washington. Washington Department of Fisheries,

617 Shellfish Division, Olympia, 44 pp.

618

619 **Goodwin, C. L., and Pease, B.** (1989). Species profiles: Life histories and environmental

620 requirements of coastal fishes and invertebrates (Pacific Northwest). Pacific geoduck clam.

621 Biological Report 82 U.S. Army Corps of Engineers and U.S. Department of the Interior, 14

622 pp.

623

624 **Green, M. A., Waldbusser, G. G., Reilly, S. L., Emerson, K. and O'Donnell, S.** (2009). Death

625 by dissolution: Sediment saturation state as a mortality factor for juvenile bivalves. *Limnology*

626 *and Oceanography* **54**, 1037–1047.

627

628 **Gurr, S. J., Rollando, C., Chan, L. L., Vadopalas, B., Putnam, H. M. and Roberts, S. B.**

629 (2018). Alternative image-based technique for phytoplankton cell counts in shellfish

630 aquaculture (no. 1001481). Nexcelom.

631

632 **Gurr, S. J., Vadopalas, B., Roberts, S. B. and Putnam, H. M.** (2020). Metabolic recovery and

633 compensatory shell growth of juvenile Pacific geoduck *Panopea generosa* following short-

634 term exposure to acidified seawater. *Conserv. Physiol.* **8**, coaa024

635

636 **Gurr, S. J., Trigg S. A., Vadopalas, B., Roberts, S. B. and Putnam, H. M.** (2020).

637 Repository for: Repeat exposure to hypercapnic seawater modifies performance and

638 oxidative status in a tolerant burrowing clam (version

639 20200622). <http://doi.org/10.5281/zenodo.3903019>

640

- 641 **Hermes-Lima, M. and Zenteno-Savín, T.** (2002). Animal response to drastic changes in oxygen
642 availability and physiological oxidative stress. *Comp. Biochem. Physiol. C.* **133**, 537–556.
643
- 644 **Hettinger, A., Sanford, E., Hill, T. M., Russell, A. D., Sato, K. N. S., Hoey, J., Forsch, M.,**
645 **Page, H. N. and Gaylord, B.** (2012). Persistent carry-over effects of planktonic exposure to
646 ocean acidification in the Olympia oyster. *Ecology* **93**, 2758–2768.
647
- 648 **Huang, X., Liu, Y., Liu, Z., Zhao, Z., Dupont, S., Wu, F., Huang, W., Chen, J., Hu, M., Lu,**
649 **W., et al.** (2018). Impact of zinc oxide nanoparticles and ocean acidification on antioxidant
650 responses of *Mytilus coruscus*. *Chemosphere* **196**, 182–195.
651
- 652 **Huo, Z., Rbbani, M. G., Cui, H., Xu, L., Yan, X., Fang, L., Wang, Y. and Yang, F.** (2019).
653 Larval development, juvenile survival, and burrowing rate of geoduck clams (*Panopea*
654 *japonica*) under different pH conditions. *Aquac. Int.* **27**, 1331–1342.
655
- 656 **Ivanina, A. V. and Sokolova, I. M.** (2016). Effects of intermittent hypoxia on oxidative stress and
657 protein degradation in molluscan mitochondria. *J. Exp. Biol.* **219**, 3794–3802.
658
- 659 **Jonsson, B. and Jonsson, N.** (2014). Early environment influences later performance in fishes. *J.*
660 *Fish Biol.* **85**, 151–188.
661
- 662 **Kapsenberg, L., Miglioli, A., Bitter, M. C., Tambutté, E., Dumollard, R. and Gattuso, J. P.**
663 (2018). Ocean pH fluctuations affect mussel larvae at key developmental transitions. *Proc.*
664 *Biol. Sci.* **285**, 20182381.
665
- 666 **Kelley, A. L., and Lunden, J. J.** (2017). Meta-analysis identifies metabolic sensitivities to ocean
667 acidification running title: ocean acidification impacts metabolic function. *Aims Environ. Sci.*
668 **4**, 709–729.
669
- 670 **Kozak, M. and Piepho, H. P.** (2018). What’s normal anyway? Residual plots are more telling
671 than significance tests when checking ANOVA assumptions. *J. Agron. Crop Sci.* **204**, 86–98.

672

673 **Kültz, D.** (2005). Molecular and evolutionary basis of the cellular stress response. *Annu. Rev.*

674 *Physiol.* **67**, 225–257.

675

676 **Kurihara, H., Kato, S. and Ishimatsu, A.** (2007). Effects of increased seawater pCO₂ on early

677 development of the oyster *Crassostrea gigas*. *Aquat. Biol.* **1**, 91–98.

678

679 **Lambert, A. J. and Brand, M. D.** (2004). Superoxide production by NADH:ubiquinone

680 oxidoreductase (complex I) depends on the pH gradient across the mitochondrial inner

681 membrane. *Biochem. J.* **382**, 511–517.

682

683 **Liao, H., Yang, Z., Dou, Z., Sun, F., Kou, S., Zhang, Z., Huang, X. and Bao, Z.** (2019). Impact

684 of ocean acidification on the energy metabolism and antioxidant responses of the yesso

685 scallop (*Patinopecten yessoensis*). *Front. Physiol.* **9**, 1967.

686

687 **Lima-Júnior, A., de Melo, D. F., Costa, J. H., Orellano, E. G., Jolivet, Y., Jarmuszkiewicz,**

688 **W., Sluse, F., Dizengremel, P. and Lima, M. S.** (2000). Effect of pH on CN-resistant

689 respiratory activity and regulation on *Vigna unguiculata* mitochondria. *Plant Physiol.*

690 *Biochem.* **38**, 765–771.

691

692 **Livingstone, D. R.** (2001). Contaminant-stimulated reactive oxygen species production and

693 oxidative damage in aquatic organisms. *Mar. Pollut. Bull.* **42**, 656–666.

694

695 **Matoo, O. B., Ivanina, A. V., Ullstad, C., Beniash, E. and Sokolova, I. M.** (2013). Interactive

696 effects of elevated temperature and CO₂ levels on metabolism and oxidative stress in two

697 common marine bivalves (*Crassostrea virginica* and *Mercenaria mercenaria*). *Comp.*

698 *Biochem. Physiol. A.* **164**, 545–553.

699

700 **Maxwell, D. P., Wang, Y. and McIntosh, L.** (1999). The alternative oxidase lowers

701 mitochondrial reactive oxygen production in plant cells. *Proc. Natl. Acad. Sci. U. S. A.* **96**,

702 8271–8276.

703

704 **McDonald, A. E. and Vanlerberghe, G. C.** (2006). Origins, evolutionary history, and taxonomic
705 distribution of alternative oxidase and plastoquinol terminal oxidase. *Comp. Biochem.*
706 *Physiol. D.* **1**, 357–364.

707

708 **McDonald, A. E., Vanlerberghe, G. C. and Staples, J. F.** (2009). Alternative oxidase in animals:
709 unique characteristics and taxonomic distribution. *J. Exp. Biol.* **212**, 2627–2634.

710

711 **Meseck, S. L., Mercaldo-Allen, R., Kuropat, C., Clark, P. and Goldberg, R.** (2018). Variability
712 in sediment-water carbonate chemistry and bivalve abundance after bivalve settlement in
713 Long Island Sound, Milford, Connecticut. *Mar. Pollut. Bull.* **135**, 165–175.

714

715 **Michaelidis, B., Ouzounis, C., Paleras, A. and Pörtner, H. O.** (2005). Effects of long-term
716 moderate hypercapnia on acid-base balance and growth rate in marine mussels *Mytilus*
717 *galloprovincialis*. *Mar. Ecol. Prog. Ser.* **293**, 109–118.

718

719 **Millenaar, F. F. and Lambers, H.** (2003). The alternative oxidase: in vivo regulation and
720 function. *Plant Biol.* **5**, 2–15.

721

722 **Miwa, S. and Brand, M. D.** (2003). Mitochondrial matrix reactive oxygen species production is
723 very sensitive to mild uncoupling. *Biochem. Soc. Trans.* **31**, 1300–1301.

724

725 **Munro, D. and Blier, P. U.** (2012). The extreme longevity of *Arctica islandica* is associated with
726 increased peroxidation resistance in mitochondrial membranes. *Aging Cell* **11**, 845–855.

727

728 **Murphy, M. P.** (2009). How mitochondria produce reactive oxygen species. *Biochem. J* **417**, 1–
729 13.

730

731 **Navarro, J. M., Torres, R., Acuña, K., Duarte, C., Manriquez, P. H., Lardies, M., Lagos, N.**
732 **A., Vargas, C. and Aguilera, V.** (2013). Impact of medium-term exposure to elevated pCO₂

733 levels on the physiological energetics of the mussel *Mytilus chilensis*. *Chemosphere* **90**,
734 1242–1248.
735
736 **Olito, C., White, C. R., Marshall, D. J. and Barneche, D. R.** (2017). Estimating monotonic rates
737 from biological data using local linear regression. *J. Exp. Biol.* **220**, 759–764.
738
739 **Pan, T.-C. F., Applebaum, S. L. and Manahan, D. T.** (2015). Experimental ocean acidification
740 alters the allocation of metabolic energy. *Proc. Natl. Acad. Sci. U. S. A.* **112**, 469
741
742 **Parker, L. M., O’Connor, W. A., Raftos, D. A., Pörtner, H.-O. and Ross, P. M.** (2015).
743 Persistence of positive carryover effects in the oyster, *Saccostrea glomerata*, following
744 transgenerational exposure to ocean acidification. *PLoS One* **10**, e0132276.
745
746 **Parker, L. M., Ross, P. M., O’Connor, W. A., Borysko, L., Raftos, D. A. and Pörtner, H.-O.**
747 (2012). Adult exposure influences offspring response to ocean acidification in oysters. *Glob.*
748 *Change Biol.* **18**, 82–92.
749
750 **Pörtner, H. O.** (2012). Integrating climate-related stressor effects on marine organisms: unifying
751 principles linking molecule to ecosystem-level changes. *Mar. Ecol. Prog. Ser.* **470**, 273–290.
752
753 **Putnam, H. M., Davidson, J. M. and Gates, R. D.** (2016). Ocean acidification influences host
754 DNA methylation and phenotypic plasticity in environmentally susceptible corals. *Evol. Appl.*
755 **9**, 1165–1178.
756
757 **Putnam, H. M., Roberts S., Spencer L. H.** (2017). Capacity or adaptation and acclimatization to
758 ocean acidification in geoduck through epigenetic mechanisms. Poster, Figshare.
759 <https://doi.org/10.6084/m9.figshare.4990889.v1>
760
761 **R Core Team** (2018). A language and environment for statistical computing.
762

- 763 **Reum, J. C. P., Alin, S. R., Feely, R. A., Newton, J., Warner, M. and McElhany, P.** (2014).
764 Seasonal carbonate chemistry covariation with temperature, oxygen, and salinity in a fjord
765 estuary: implications for the design of ocean acidification experiments. *PLoS ONE* **9**, e89619.
766
- 767 **Ristow, M. and Schmeisser, K.** (2014). Mitohormesis: promoting health and lifespan by increased
768 levels of reactive oxygen species (ROS). *Dose-Response* **12**, dose–response.1.
769
- 770 **Roberts, S., White, S., Trigg, S. A., and Putnam, H.M.** (2020). *Panopea_generosa_genome*.
771 OSF. June 24. doi:10.17605/OSF.IO/YEM8N.
772
- 773 **Shamshak, G. L., and King, J. R.** (2015). From cannery to culinary luxury: the evolution of the
774 global geoduck market. *Mar. Policy* **55**: 81–89.
775
- 776 **Slocinska, M., Barylski, J. and Jarmuszkiewicz, W.** (2016). Uncoupling proteins of
777 invertebrates: A review. *IUBMB Life* **68**, 691–699.
778
- 779 **Sokolova, I. M.** (2013). Energy-limited tolerance to stress as a conceptual framework to integrate
780 the effects of multiple stressors. *Integr. Comp. Biol.* **53**, 597–608.
781
- 782 **Sokolova, I. M., Frederich, M., Bagwe, R., Lannig, G. and Sukhotin, A. A.** (2012). Energy
783 homeostasis as an integrative tool for assessing limits of environmental stress tolerance in
784 aquatic invertebrates. *Mar. Environ. Res.* **79**, 1–15.
785
- 786 **Strahl, J., Brey, T., Philipp, E. E. R., Thorarinsdóttir, G., Fischer, N., Wessels, W. and Abele,**
787 **D.** (2011). Physiological responses to self-induced burrowing and metabolic rate depression in
788 the ocean quahog *Arctica islandica*. *J. Exp. Biol.* **214**, 4223–4233.
789
- 790 **Sussarellu, R., Dudognon, T., Fabioux, C., Soudant, P., Moraga, D. and Kraffe, E.** (2013).
791 Rapid mitochondrial adjustments in response to short-term hypoxia and re-oxygenation in the
792 Pacific oyster, *Crassostrea gigas*. *J. Exp. Biol.* **216**, 1561–1569.
793

- 794 **Tanner, R. L. and Dowd, W. W.** (2019). Inter-individual physiological variation in responses to
795 environmental variation and environmental change: Integrating across traits and time. *Comp.*
796 *Biochem. Physiol. A.* **238**, 110577.
797
- 798 **Timmins-Schiffman, E., Guzmán, J. M., Thompson, R. E., Vadopalas, B., Eudeline, B. and**
799 **Roberts, S. B.** (2019). Dynamic response in the larval geoduck (*Panopea generosa*) proteome
800 to elevated pCO₂. *Ecol. Evol.* **10**, 185–197.
801
- 802 **Tomanek, L., Zuzow, M. J., Hitt, L., Serafini, L. and Valenzuela, J. J.** (2012). Proteomics of
803 hyposaline stress in blue mussel congeners (genus *Mytilus*): implications for biogeographic
804 range limits in response to climate change. *J. Exp. Biol.* **215**, 3905–3916.
805
- 806 **Tomanek, L., Zuzow, M. J., Ivanina, A. V., Beniash, E. and Sokolova, I. M.** (2011). Proteomic
807 response to elevated PCO₂ level in eastern oysters, *Crassostrea virginica*: evidence for
808 oxidative stress. *J. Exp. Biol.* **214**, 1836–1844.
809
- 810 **Tschischka, K., Abele, D. and Pörtner, H. O.** (2000). Mitochondrial oxyconformity and cold
811 adaptation in the polychaete *Nereis pelagica* and the bivalve *Arctica islandica* from the Baltic
812 and White Seas. *J. Exp. Biol.* **203**, 3355–3368.
813
- 814 **Vanlerberghe, G. C.** (2013). Alternative oxidase: a mitochondrial respiratory pathway to maintain
815 metabolic and signaling homeostasis during abiotic and biotic stress in plants. *Int. J. Mol. Sci.*
816 **14**, 6805–6847.
817
- 818 **Visser, B., Williams, C. M., Hahn, D. A., Short, C. A. and López-Martínez, G.** (2018).
819 Hormetic benefits of prior anoxia exposure in buffering anoxia stress in a soil-pupating insect.
820 *J. Exp. Biol.* **221**, jeb167825.
821
- 822 **Waldbusser, G. G., Hales, B., Langdon, C. J., Haley, B. A., Schrader, P., Brunner, E. L.,**
823 **Gray, M. W., Miller, C. A. and Gimenez, I.** (2015). Saturation-state sensitivity of marine
824 bivalve larvae to ocean acidification. *Nat. Clim. Change* **5**, 273–280.

825

826 **Walsh, P. J. and Louise Milligan, C.** (1989). Coordination of metabolism and intracellular acid–
827 base status: ionic regulation and metabolic consequences. *Can. J. Zool.* **67**, 2994–3004.

828

829 **White, M. M., McCorkle, D. C., Mullineaux, L. S. and Cohen, A. L.** (2013). Early exposure of
830 bay scallops (*Argopecten irradians*) to high CO₂ causes a decrease in larval shell growth.
831 *PLoS ONE* **8**, e61065.

832

833 **Wojtczyk-Miaskowska, A. and Schlichtholz, B.** (2018). DNA damage and oxidative stress in
834 long-lived aquatic organisms. *DNA Repair* **69**, 14–23.

835

836 **Yusseppone, M. S., Rocchetta, I., Sabatini, S. E., Luquet, C. M., de Molina, M. del C. R.,**
837 **Held, C. and Abele, D.** (2018). Inducing the alternative oxidase forms part of the molecular
838 strategy of anoxic survival in freshwater bivalves. *Front. Physiol.* **9**, 100.

839

840 **Zhang, Y., Humes, F., Almond, G., Kavazis, A. N. and Hood, W. R.** (2018). A mitohormetic
841 response to pro-oxidant exposure in the house mouse. *Am. J. Physiol. Regul. Integr. Comp.*
842 *Physiol.* **314**, R122–R134.